Received: 28 November 2018 | Revised: 3 July 2019 | Accepted: 4 July 2019

DOI: 10.1002/dep2.79

ORIGINAL RESEARCH ARTICLE

The Depositional Record Open Access
A journal of the International Association of Sedimentologists
WILEY

Terrestrial microbialites provide constraints on the mesoproterozoic atmosphere

Michael T. Hren[1,2] | **Nathan D. Sheldon**[3]

[1]Center for Integrative Geosciences, University of Connecticut, Storrs, Connecticut

[2]Department of Chemistry, University of Connecticut, Storrs, Connecticut

[3]Department of Earth & Environmental Sciences, University of Michigan, Ann Arbor, Michigan

Correspondence
Michael T. Hren, Center for Integrative Geosciences, University of Connecticut, Storrs, CT.
Email: hren@uconn.edu

Funding information
University of Michigan; NSF EAR, Grant/Award Number: 1050760

Abstract

Palaeoclimate data indicate that Earth surface temperatures have remained largely temperate for the past 3.5 Byr despite significantly lower solar luminosity over this time relative to the present day. There is evidence for episodic early and late Proterozoic glaciation, but little evidence of glaciation in the intervening billion years. A prolonged equable Mesoproterozoic Earth requires elevated greenhouse gas concentrations. Two endmember scenarios have been proposed for maintaining global warmth. These include extremely high pCO_2 or more modest pCO_2 with higher methane concentrations. This paper reports on the $\delta^{13}C$ of organic matter in 1.1 Ga stromatolites from the Copper Harbor Conglomerate (CHC) of the Mesoproterozoic Midcontinent Rift (North America) and $\delta^{18}O$ and Δ_{47} temperatures of inorganic stromatolite carbonate to constrain formation and burial conditions and the magnitude of ancient carbon isotope discrimination. CHC sediments have never been heated above ~125–155°C, providing a novel geochemical archive of the ancient environment. Stromatolite Δ_{47} data record moderate alteration, and therefore, the occluded organic matter was unlikely to have experienced significant thermal alteration after deposition. The $\delta^{13}C$ values of ancient mat organic matter and inorganic carbonate show isotope discrimination (ε_p) values ~15.5–18.5‰, similar to modern microbial mats formed in equilibrium with low concentrations of dissolved inorganic carbon. In combination, these data are consistent with a temperate climate Mesoproterozoic biosphere supported by relatively modest pCO_2. This result agrees with Atmosphere-Ocean Global Circulation Model reconstructions for Mesoproterozoic climate using 5–10 times present atmospheric levels pCO_2 and pCH_4 of >28 ppmv. However, given marine modelling constraints of CH_4 production that suggest pCH_4 was below 10 ppm, this creates a methane paradox. Either an additional source of CH_4 (e.g. from terrestrial ecosystems) or another greenhouse gas, such as N_2O, would have been necessary to maintain equable conditions in the Mesoproterozoic.

KEYWORDS

clumped Isotopes, Mesoproterozoic, mid-continent rift system, pCO_2, stromatolites

1 | INTRODUCTION

Constraints on Earth surface temperature and atmospheric composition provide critical insight regarding the evolution of the biosphere (Kasting, 1993). The Mesoproterozoic has long been considered to be part of the 'boring billion' years between the Palaeoproterozoic Huronian and Neoproterozoic 'snowball Earth' events, when there was comparatively little change in Earth surface, greenhouse gas or oceanic conditions (Shields and Veizer, 2002; Lyons *et al.*, 2014; Planavsky *et al.*, 2014) accompanied by relatively steady atmospheric pO_2. More recently, however, new data indicate complex patterns of oceanic oxygenation and euxinia through time (Planavsky *et al.*, 2014, 2018) and suggest that by the mid-Proterozoic, atmospheric pCO_2 likely dropped to less than one quarter of the Palaeoproterozoic levels (Kaufman and Xiao, 2003; Sheldon, 2006, 2013). For example, Kanzaki and Murakami (2015) estimate 23–210 times present atmospheric levels (PAL) at 1.85 Ga based on palaeosol geochemistry, but a number of studies have estimated the pCO_2 of the Mesoproterozoic (Kaufman and Xiao, 2003; Bartley and Kah, 2004; Kah and Riding, 2007; Mitchell and Sheldon, 2010) and report widely varying, but generally much lower estimates. For example, Kaufman and Xiao (2003) give an estimate of 10–200 PAL pCO_2 at 1.4 Ga based on the carbon isotopic composition of large microfossils, Kah and Riding (2007) give an estimate of ≤10 PAL at 1.2 Ga based on microbialite sheath calcification and a number of palaeosols from the Midcontinent Rift (Mitchell and Sheldon, 2010; Sheldon, 2013) have consistently indicated 4–6 PAL at 1.1 Ga. A fundamental question is whether or not pCO_2 of this range could maintain temperate, non-glacial conditions without an additional greenhouse gas present. Given that a variety of proxies are consistent with low atmospheric pO_2 in the Mesoproterozoic (reviewed in Planavsky *et al.*, 2018), CH_4 would likely have been stable in the atmosphere, and given that it has a warming potential about 25 times that of CO_2, it has often been proposed as a candidate Proterozoic greenhouse gas (Sheldon, 2013).

However, recent work suggests that anaerobic oxidation of CH_4 coupled with SO_4^{2-} reduction may have limited the flux of CH_4 from marine systems and potentially limited the buildup of CH_4 in the Proterozoic atmosphere (Olson *et al.*, 2016). If this is correct, higher pCO_2 or elevated amounts of some other additional greenhouse gas would be needed to maintain temperate conditions. Constraints from the rock record (see supplemental table DR1 from Fiorella and Sheldon, 2017) indicate no evidence for glaciation at this time, except at one locality, to at least 60° N and S. New Atmospheric-Ocean Global Circulation Model (AOGCM) results show that the modest (5–10 PAL) concentrations of CO_2 could maintain a largely ice-free globe with a range of pCH_4 from 28 to 280 ppmv (Fiorella and Sheldon, 2017), although a completely ice-free globe is only possible at the highest total greenhouse gas loads. Thus, Zhao *et al.* (2017) have described the late Mesoproterozoic as a potential methane paradox.

Morphological evidence for microbialite abundance and diversity indicate maxima for both during the Mesoproterozoic (Noffke and Awramik, 2013). Some argue that this is due to the evolution of new carbonate concentration mechanisms in the sheaths of cyanobacteria (Riding, 2011) that could have evolved in response to changing atmospheric conditions. Continental environments might have been even more chemically favourable for habitation than marine environments (Parnell *et al.*, 2015) at this time. A range of evidence supports episodic glaciation during the early and late Proterozoic (Kaufman *et al.*, 1997; Kennedy *et al.*, 1998; Walter *et al.*, 2000; Kendall *et al.*, 2004), but there is little or no evidence of prolonged, widespread glaciation during the Mesoproterozoic (table S1 of Fiorella and Sheldon, 2017). Thus, the inferred increase in microbialite abundance and diversity occurs during a time of clement conditions and of broad potential ecological niches including marine (Kah *et al.*, 1999), transitional (Beghin *et al.*, 2017) and terrestrial environments (Wellman and Strother, 2015). In total, biological and sedimentological evidence suggest a robust biosphere with globally temperate, ice-free conditions during this prolonged interval. If the Mesoproterozoic was a period of general and prolonged warmth, was high CO_2 responsible for the lack of glaciation?

This study presents new clumped and organic isotopic analyses of low thermal maturity stromatolites from Horseshoe Harbor, Michigan, within the Copper Harbor Conglomerate (CHC) of the Mesoproterozoic-aged Midcontinent Rift. Recent work demonstrates that these mats and associated geologic formations are minimally altered and have experienced limited heating in the 1.1 Byr since deposition (Nishioka, 1984; Gallagher *et al.*, 2017). Clumped isotope temperatures provide some constraint on maximum formation temperatures and the potential for burial alteration of the organic isotopes, making it possible to use paired records of organic and inorganic carbon isotopes as a semi-quantitative indicator of atmospheric gas concentration.

2 | GEOLOGIC SETTING

2.1 | Midcontinent Rift System

The Midcontinent Rift System (MCR; Figure 1) represents a widespread, failed continental rifting event that is characterized by large-scale emplacement of flood basalts that occurred in multiple pulses of volcanism ~1.1 Ga (Davis and Paces, 1990; Hutchinson *et al.*, 1990; Ohr, 1993; Cumming *et al.*, 2013). Rifting and extension are associated with widespread sedimentary deposition during early rift subsidence and record a classic continental rift sequence of alluvial

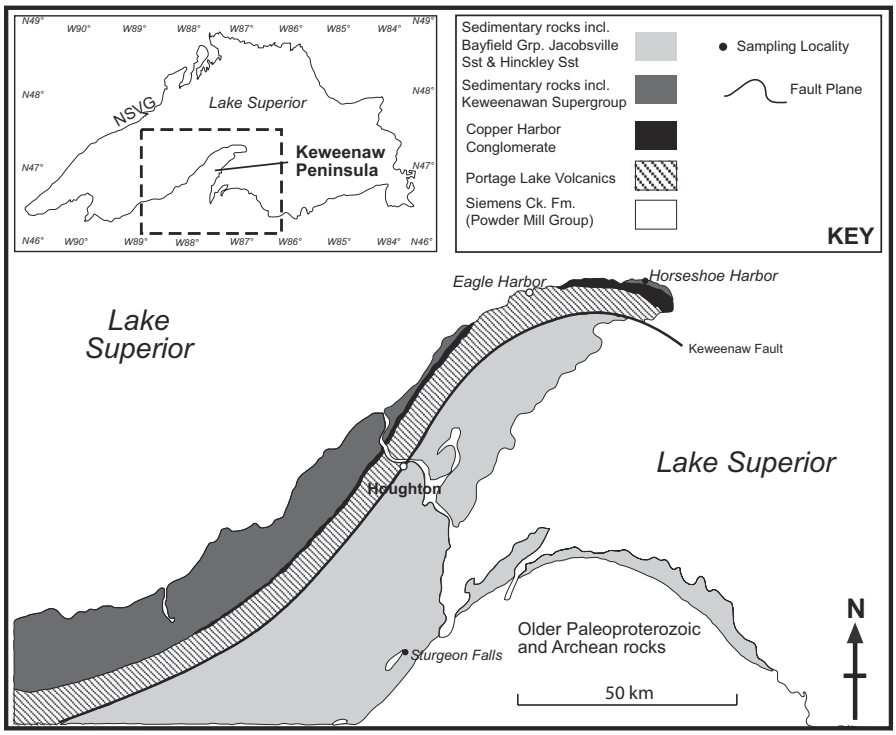

FIGURE 1 Location map for Copper Harbor Conglomerate on the Keweenaw Peninsula, Michigan, USA. Samples were collected from Horseshoe Harbor and pCO_2 estimates from that site are compared to estimates from a palaeosol at Sturgeon Falls (MI) and from palaeosols in the North Shore Volcanic Group (NSVG; inset map). Figure modified after Mitchell and Sheldon (2016)

fan sediments that transition to lacustrine and fluvial systems (Elmore *et al.*, 1989; Mitchell and Sheldon, 2009, 2016). These igneous and clastic sedimentary units are collectively referred to as the Keweenaw Supergroup (Morey and Ojakangas, 1982). On the eastern side of the rift, this includes lower volcanic strata through sedimentary strata of the Oronto Group, terminating in overlying sandstone units.

In Michigan (USA), the clastic sediments of the Oronto Group consist of the CHC, Nonesuch and Freda formations, corresponding to the alluvial fan, lacustrine and fluvial deposits that span the rift interval (Elmore, 1984, Elmore *et al.*, 1989).The main stage of the MCR (Figure 1) occurred over a period of less than 50 Myr (Cannon and Hinze, 1992) and rifting was soon followed by regional compression that drove reactivation and reversal of rift-bounding faults (Stein *et al.*, 2015) associated with uplift of rift sediments. The rapid process of rifting and resultant regional compression means that rift sediments (Figure 1) were shallowly buried and minimally heated in some parts of the rift (<125°C; Mauk and Hieshima, 1992). This is due to the absence of large regional tectonic deformation in the mid-continent and the relatively short duration of rifting (Pratt *et al.*, 1991; Price *et al.*, 1996). The MCR experienced prehnite–pumpellyite grade metamorphism in places close to the basin-bounding faults, but thermal history models of available temperature constraints from the Nonesuch and CHC formations within the MCR indicate both low peak burial temperatures and a relatively short duration of burial before unroofing (Gallagher *et al.*, 2017). Fluid inclusion studies of CHC microbial mats show that isolated inclusions homogenize at temperatures as low as 53–88°C (Nishioka *et al.*, 1984). These low temperatures contrast with fluid inclusion data from carbonates directly associated with copper mineralization that show homogenization temperatures up to 119°C (Livnat, 1983). Thus, Nonesuch and CHC localities that are away from basin-bounding faults typically experienced relatively mild thermal alteration to temperatures well below experimental constraints for abiotic Fischer–Tropsch synthesis of organic compounds (i.e. 250°C, high pressure; McCollom and Seewald, 2006, Taran *et al.*, 2007).

2.2 | Evidence for Life and Temperate Conditions in the MCR

The MCR extends from Kansas to Ontario and preserves a variety of textural evidence for life (Noffke, 2009; Sheldon, 2012; Noffke and Awramik, 2013; Wilmeth *et al.*, 2014) that support the interpretations of a widely distributed terrestrial biosphere at 1.1 Ga (Figures 2 and 3). This includes a number of fossil-bearing lake (Wellman and Strother, 2015), pond (Elmore, 1983) and floodplain deposits (Sheldon, 2012) that preserve an array of acritarchs, stromatolites and microbially induced sedimentary structures. The stromatolites are found primarily in the CHC at two localities, and are interpreted to have formed in the distal parts of an alluvial fan where braided streams emptied into a large lake system associated with the Nonesuch Formation shale and mudstone deposition (Figure 2). These sediments display similarities to modern playa mudflats (Nishioka *et al.*, 1984) and

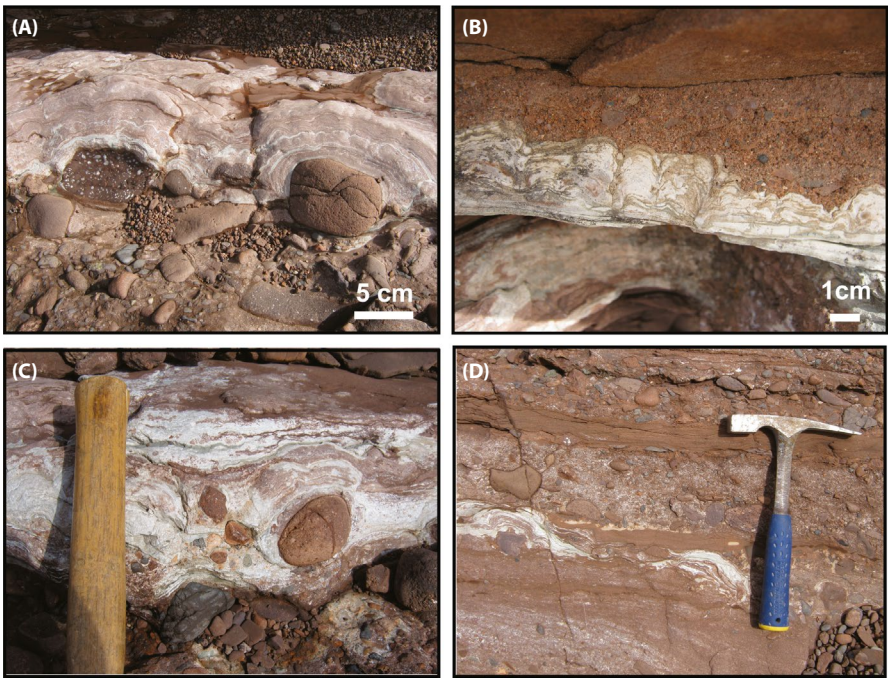

FIGURE 2 Field photos of Copper Harbor Conglomerate stromatolites. Image of (A) stromatolite mats growing on large cobbles, (B) infilled by coarse-grained sands, (C) with cobbles and gravel entrained within the mat and (D) growing on cobbles and sandy beds and with entrained sand layers

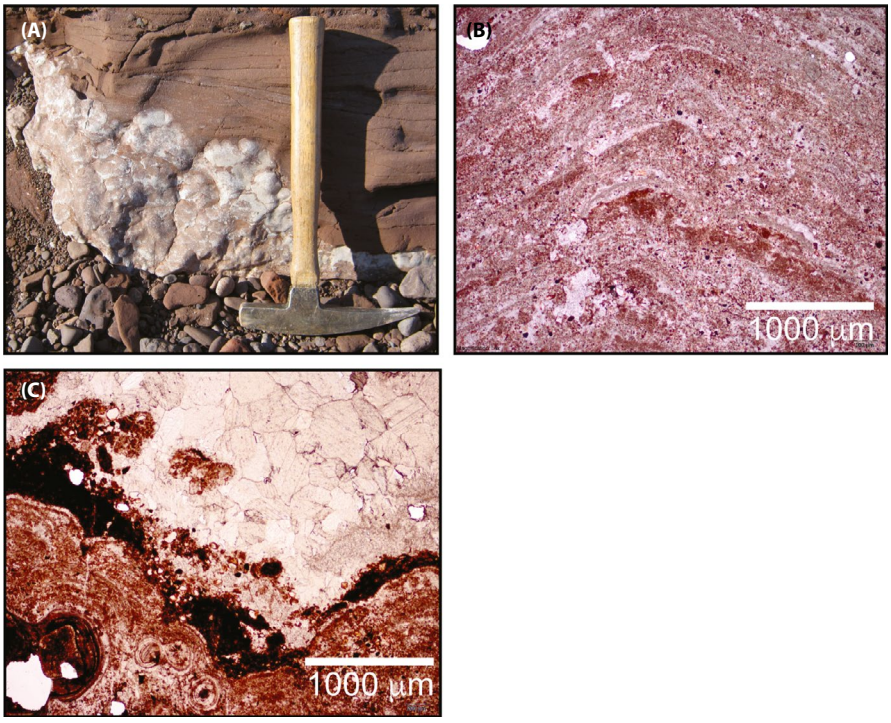

FIGURE 3 Field and thin section photos of Copper Harbor Conglomerate stromatolites. (A) Stromatolite mat overlain by coarse-grained sandstone deposited in a fluvial setting. (B) Thin-section image of finely laminated mat with mineral grains embedded in the mat matrix. (C) Thin section image of the top of a mat layer, bounded by secondary sparite

preserve evidence of desiccation features in both mudflat/sandflat and braidplain facies (Fedorchuk *et al.*, 2016). Stromatolitic structures show alternation between detrital and carbonate laminae (Figures 2 and 3), with radial calcite overgrowths in some areas of the laminae (Elmore, 1983), and both abiogenic and biogenic forms have been identified (Fedorchuk *et al.*, 2016). Both within the CHC (Wilmeth *et al.*, 2014) and elsewhere within the MCR (Sheldon, 2012), other domal microbialite features have been noted, including some with preserved organic matter, suggesting a wide array of potential microbial communities and inhabited environmental niches at this time. Previous workers have demonstrated the potential for using the clumped isotope composition of similar microbialites in the geologic record to reconstruct environmental conditions at the time of their formation in lake and lake-margin deposits. These studies show that modern and ancient microbial carbonates reasonably record the temperature of

the past surface water conditions, though they may be biased by variations in timing of precipitation or formation depths (Frantz *et al.*, 2014; Petryshyn *et al.*, 2015).

3 | METHODS

Stromatolites within CHC sediments at Horseshoe Harbor contain both calcitic laminae preserved in fine growth layers and sparite present in in-filled voids and larger, secondary fractures (Elmore, 1983, 1984). Samples were collected from the CHC in 2011, cut using a solvent-cleaned, water-cooled rock saw and polished using a diamond grit polish. Thin sections were analysed to identify areas with no or minimal alteration of primary laminae. Samples of pristine carbonate laminae and secondary sparite were drilled at low speed using a Micromill to evaluate potential spatial variability in isotopic data. Drilled areas were specifically chosen to minimize any potential contamination with visible secondary carbonate. This had the effect of limiting the sample size available for analysis. Carbonate powders were reacted with 105% anhydrous phosphoric acid in a common acid bath at the University of Michigan (UM) and analysed for $\delta^{13}C$, $\delta^{18}O$ and Δ_{47} on a Thermo Scientific MAT 253 Mass Spectrometer following established extraction and data reduction procedures (Defliese *et al.*, 2015; Methods S1). For organic $\delta^{13}C$, carbonate was removed via reaction with weak HCl and analysed at UM on a Costech Elemental Analyzer attached to a Thermo Delta V. The Δ_{47} values were corrected for the temperature of acid reaction (Defliese *et al.*, 2015) and normalized relative to the Absolute Reference Frame of Dennis *et al.* (2011). Stromatolitic material contains a relatively high abundance of organic matter that can pose a challenge to reliable clumped isotope measurements. Analytical methods ensured samples presented had low Δ_{48} and Δ_{49} values. Isotopic data are included in Tables 1–3. Mean Δ_{47} values of UM Carrara after normalization were 0.397 ± 0.007 and 0.406 ± 0.007 during the analytical period. SEs for Δ_{47} temperature estimates were ~2.6 to 6°C for unknowns, with the exception of two samples that show considerably higher uncertainty (11.7°C), possibly due to heterogeneity of the carbonate powder as a result of inclusion of trace amounts of secondary, higher temperature sparite during the micro-drilling process. Reproducibility for conventional carbonate $\delta^{13}C$ and $\delta^{18}O$ and organic carbon $\delta^{13}C$ was better than 0.2‰ for all analyses. All of the measured and calculated geochemical data are presented in Tables 1–3 and raw data in Data S1. All data were collected prior to the establishment of current background and ^{17}O correction procedures (Bernasconi *et al.*, 2018; Peterson *et al.*, 2019), which can result in higher analytical uncertainties than present.

4 | RESULTS

4.1 | Carbonate geochemistry results

Thin section analyses of mat carbonates show finely laminated layers (Figure 3B,C) with organic matter bound, in parts, by coarse-grained, anhedral microsparite that is readily distinguished from laminated carbonate. Stromatolite microfabrics contain light–dark laminae ~20 μm to several millimetres thick and consist of calcite and a mix of detrital material (Elmore, 1983, 1984). Mean mat Δ_{47} values range from 0.602 to 0.699, corresponding to temperatures of 22–44°C for the Defliese *et al.* (2015) calibration line (Table 1), which was derived in the Stable Isotope Lab at UM. For reference, temperatures calculated for the same Δ_{47} values were calculated following the Dennis *et al.* (2011) calibration line as well (Table 1). The Δ_{47} values for anhedral sparite are lower (0.568–0.666), yielding higher formation temperatures of 29–54°C (Defliese *et al.*, 2015). These data show a consistent, but small offset between primary and secondary carbonate Δ_{47}, indicating infilling of void space by secondary calcite after burial. Secondary carbonate may bias primary carbonate material via infilling of microvoids in the carbonate fabric that may be difficult to separate when sampling. The Δ_{47} temperatures are used for two purposes: (a) to provide constraints on potential diagenetic temperatures affecting organic carbon associated with the mats and (b) to provide reasonable bounds to calculate the $\delta^{18}O$ of fluids in equilibrium with the carbonate using the temperature-dependent fractionation factor (Kim and O'Neil, 1997). Δ_{47} temperatures may also provide an upper bound for formation temperature, as secondary processes are unlikely to produce cooler temperatures. The Δ_{47} temperatures and $\delta^{18}O_{carb}$ yield water compositions of −1.7 to −5.4‰ for T°C = 25 and 40°C (Table 3), consistent with a range of fresh meteoric waters at low latitude, although calculated fluid compositions have the potential to be biased by any post-depositional solid-state bond reordering that could have affected clumped isotope temperatures.

4.2 | Organic geochemistry results

Copper Harbor Conglomerate stromatolites contain 0.04–0.22 wt% organic carbon within carbonate laminae. In areas with no visible recrystallization, it is assumed that this organic matter reflects primary Mesoproterozoic organics, unmodified by any post-depositional thermal processes (see "Preservation potential of Carbonate Δ_{47} During Burial and Sediment Diagenesis"). The $\delta^{13}C_{org}$ values range from −24.0 to −27.4‰ (Table 2) and are comparable to $\delta^{13}C_{org}$ from contemporaneous floodplain sedimentary rocks from the MCR (−26 to −29‰; Sheldon, 2012) and enriched compared to Nonesuch Formation kerogen ($\delta^{13}C$ = −30 to −34‰; Imbus *et al.*, 1992). Inorganic

TABLE 1 Δ_{47} data for stromatolite growth bands and sparite crystals

Sample	Δ_{47}	$\delta^{13}C$	$\delta^{18}O_{Raw}$	Δ_{47}	HG slope	Slope[a]	Intercept[b]	Δ_{47}	*T* (°C)[c]	Mean *T* (°C)	*SE*	*T* (°C)[d]	Mean *T* (°C)	*SE*
A	−8.99	−1.69	31.41	0.009	0.0254	1.0989	1.020	0.596	52			46		
A	−10.73	−1.65	30.13	0.009	0.0254	1.0989	1.020	0.616	47	50	2.7	40	43	2.6
A_2	−7.12	−2.54	31.93	0.040	0.0311	1.0611	0.923	0.754	16			11		
A_2	−5.73	−1.38	32.26	0.033	0.0311	1.0611	0.923	0.645	40	28	11.7	34	22	11.5
B	−7.40	−1.42	31.75	0.012	0.0254	1.0989	1.020	0.661	36			30		
B	−4.80	−1.13	32.45	0.012	0.0254	1.0989	1.020	0.648	39			33		
B	−3.52	−1.36	32.37	0.007	0.0254	1.0989	1.020	0.612	48	41	3.7	42	35	3.7
C	−7.85	−1.31	31.64	0.009	0.0254	1.0989	1.020	0.595	53			46		
C	−7.15	−1.13	31.81	0.006	0.0254	1.0989	1.020	0.588	54			48		
C	−6.66	−1.10	32.04	0.010	0.0254	1.0989	1.020	0.622	45	51	3.6	39	44	3.6
D	−8.72	−1.37	31.61	0.026	0.0269	1.0586	1.059	0.677	32			26		
D	−8.96	−1.37	31.56	0.025	0.0311	1.0611	0.923	0.615	47	40	7.4	41	34	7.3
A_sparite	−7.13	−1.63	31.14	0.013	0.0254	1.0989	1.020	0.608	49			43		
A_sparite	−7	−1.31	32.29	0.023	0.0311	1.0611	0.923	0.528	72	61	11.7	66	54	11.4
B_Sparite	−6.59	−1.33	32.27	0.021	0.0269	1.0586	1.059	0.654	38			31		
B_Sparite	−8.97	−1.25	31.87	0.025	0.0269	1.0586	1.059	0.623	45	41	3.8	39	35	3.7

[a]Transfer function slope.

[b]Transfer function intercept.

[c]Calculated temperature using Ghosh *et al.*, 2006 temperature equation adjusted to the ARF after Dennis *et al.* (2011).

[d]Calculated temperature using Defliese *et al.* (2015).

TABLE 2 Organic carbon data

	$\delta^{13}C$	Weight %
Stromatolite		
MI-UP-P	−24.0	0.140
MI-UP-Q	−25.5	0.043
MI-UP-S	−27.4	0.199
MI-UP-T	−26.3	0.106
Matrix carbonate		
MI-UP-O	−25.0	0.184
MI-UP-R	−26.0	0.219

carbonate $\delta^{13}C$ values from stromatolite laminae range from −0.8 to −1.9‰ with $\delta^{18}O$ of 23.2 to 24.1‰ VPDB and show little or no variability with position in the mat. Measured CHC carbonate $\delta^{13}C$ values are consistent with $\delta^{13}C_{carb}$ values of carbonates found within the Nonesuch shale and CHC mat carbonates (Imbus *et al.*, 1992). Imbus *et al.* (1992) note that consistency between CHC mat carbonate $\delta^{13}C$ and Nonesuch layered carbonate $\delta^{13}C$ suggests a common Dissolved Inorganic Carbon (DIC) source for these associated sediments.

5 | DISCUSSION

5.1 | Preservation potential of Carbonate Δ_{47} During Burial and Sediment Diagenesis

The Δ_{47} data from mat carbonates have the potential to record Mesoproterozoic temperature; however, there are a number of potentially significant uncertainties associated with interpreting Δ_{47} data from 1.1 Ga microbial carbonates. This is particularly true when relating measured temperature to environmental conditions at the time of mat formation. Thus, it is suggested that measured Δ_{47} temperatures do not necessarily reflect primary formation temperature, but could record a combination of formation temperature plus secondary effects that bias primary signatures. First, a number of authors have identified deviations from the experimental temperature-Δ_{47} calibration line for equilibrium precipitation (Ghosh *et al.*, 2006) that may result from kinetic isotope effects (Ghosh *et al.*, 2006; Affek *et al.*, 2008; Tripati *et al.*, 2010; Daëron *et al.*, 2011; Saenger *et al.*, 2012; Eagle *et al.*, 2013). This has the potential to influence interpreted carbonate formation temperature. If mat carbonate forms at or near equilibrium, Δ_{47} from CHC mats should yield reliable temperature estimates, barring secondary alteration or solid-state reordering. However, if the carbonates formed via rapid CO_2 degassing (Affek *et al.*, 2008), kinetic effects could decrease recorded Δ_{47} values, producing an increase in apparent temperature. Recent work by Petryshyn *et al.* (2016) shows that modern microbial mats yield Δ_{47} temperatures within error of summer water temperature for non-diagenetically altered carbonates. However, ancient mat carbonates from the Eocene Green River Formation (Frantz *et al.*, 2014) are also shown to reproduce surface water temperatures reasonably well. Thus, while the extent of kinetic bias on temperature relationships are at present unknown, microbial carbonate temperatures recorded by carbonate Δ_{47} are generally consistent with modern environmental conditions, but represent at best a seasonal maximum. This result is similar to Δ_{47} in other lacustrine carbonates that are shown to record warm season temperatures (Hren and Sheldon, 2012).

TABLE 3 Calculated carbon isotope discrimination for CHC mats

			25°C	40°C	25°C	40°C	25°C	40°C
Sample (stromatolite)	$\delta^{13}C$	$\delta^{18}O$	Calculated $\delta^{13}C_{CO_{2aq}}$ [b]	Calculated $\delta^{13}C_{CO_{2aq}}$ [b]	ε_p [c]	ε_p [d]	ε_p [c]	ε_p [d]
CH-A	−1.4	23.2	−11.1	−9.9	16.7	15.1	18.0	16.3
CH-B	−1.2	23.9	−10.9	−9.7	17.0	15.3	18.2	16.5
CH-C	−1.2	23.9	−10.9	−9.7	16.9	15.3	18.2	16.5
CH-D	−1.2	23.8	−10.9	−9.7	16.9	15.3	18.2	16.5
CH-F	−1.2	23.7	−11.0	−9.8	16.9	15.2	18.1	16.5
CH-I	−0.9	23.7	−10.6	−9.4	17.2	15.6	18.5	16.8
CH-J	−0.9	23.7	−10.6	−9.4	17.3	15.6	18.5	16.9
CH-K	−0.8	23.9	−10.5	−9.3	17.4	15.7	18.6	17.0
CH-L	−0.8	24.1	−10.5	−9.3	17.3	15.7	18.6	16.9
CH-M	−0.9	23.7	−10.7	−9.5	17.2	15.5	18.4	16.8
Mean	−1.1	23.8	−10.8	−9.6	17.1	15.4	18.3	16.7

[a] Δ_{47} Temperature (°C).

[b] Calculated $\delta^{13}C_{CO_{2aq}}$ using the temperature specified and the temperature dependent $\alpha_{calcite\text{ - }CO_{2aq}}$ of Deines *et al.* (1974)

[c] $\varepsilon_p = 1000\ (\delta^{13}C_{CO_2} - \delta^{13}C_p)/(1000+\delta^{13}C_p)$ after Laws *et al.* (1995) using the minimum $\delta^{13}C_{org}$ as δ_p.

[d] $\varepsilon_p = 1000\ (\delta^{13}C_{CO_2} - \delta^{13}C_p)/(1000+\delta^{13}C_p)$ after Laws *et al.* (1995) using the mean $\delta^{13}C_{org}$ as δ_p.

Second, solid-state bond reordering has the potential to alter Δ_{47} values over 1.1 Ga and at moderate temperatures (Henkes *et al.*, 2014). This becomes a greater probability with increasing burial temperature and time. Thus, Δ_{47} values from Proterozoic carbonates should be viewed cautiously as a record of primary *T* °C and most likely represents a combination of primary temperatures and an unknown degree of thermal reordering. For CHC stromatolites, potential post-depositional Δ_{47} alteration is likely minimized by low burial depths and temperatures. The coolest stromatolitic Δ_{47} temperatures measured are <30°C and mean sparite Δ_{47} temperatures are all lower than 54°C. Clumped isotope temperatures therefore likely show minor thermal alteration during shallow burial heating since the Mesoproterozoic. Biomarker and clay mineral thermometry support low regional MCR burial temperatures (100–125°C) (Nishioka *et al.*, 1984; Pratt *et al.*, 1991), but far warmer than measured mat Δ_{47} values. Regional temperatures from clay and biomarker data are consistent with recent clumped isotope results from the MCR White Pine Mine, that show spatially variable hydrothermal temperatures (49–116°C) in association with zones of copper mineralization, and fluid inclusions show equilibration temperatures of 53–88°C (Nishioka *et al.*, 1984). If the MCR experienced prolonged periods of high temperature (>125°C) for tens of millions of years, this could have the effect of resetting primary Δ_{47} results to lower values (higher *T* °C) (Gallagher *et al.*, 2017). The highest measured Δ_{47} temperatures in the MCR are found in areas with obvious alteration of primary carbonate and closest to the major bounding Keweenaw Fault. Results from altered CHC carbonates relatively close to the Keweenaw Fault show the lowest Δ_{47} temperatures of the MCR even within the alteration zone (~70°C; Gallagher *et al.*, 2017). The sample location of Horseshoe Harbor, well-removed from the Keweenaw Fault, suggests that it is within one of the lowest thermal alteration zones of the whole MCR and thus would be expected to have the least thermal impact from either burial or primary ore-related fluids. This is supported by fluid inclusion data that show the lowest closure temperatures are found within mat carbonates at Dan's point, near the sampling locality used for this paper (Nishioka *et al.*, 1984). In the absence of recrystallization, post-depositional alteration is expected to decrease bond ordering (Henkes *et al.*, 2014) and Δ_{47} values, resulting in higher calculated temperatures. Bond-reordering experiments predict that the Δ_{47} temperatures preserved by stromatolites could in fact reflect primary or early diagenetic crystallization temperature (Henkes *et al.*, 2014; Shenton *et al.*, 2015). Regardless, the low temperatures recorded in mat carbonate Δ_{47} suggest minimal temperature effects due to bond reordering.

In addition to the effects of bond reordering, shallow-water carbonate diagenesis can introduce alteration of primary geochemical signatures within ancient carbonates (Ahm *et al.*, 2018; Higgins *et al.*, 2018). In particular, variations in the extent and style of early diagenesis can influence whether the composition of the carbonate mineral is determined by chemistry of the fluid or by the precursor sediment. This results from the fact that the transformation of metastable carbonate minerals to more recalcitrant forms, such as limestone or dolomite, involves exchange between mineral and pore fluids that can translate to fluid-buffered exchange for one element such as O and sediment buffered for another such as C (Higgins *et al.*, 2018). Indeed, Swart (2008) argues that stratigraphic variations in Neogene marine carbonate $\delta^{13}C$ could be explained, in part, due to mixing of pelagic and platform C sources with distinct $\delta^{13}C$ values. Higgins *et al.* (2018) suggest that observed Neogene carbonate $\delta^{13}C$ trends could reflect changes in the extent of diagenetic alteration of aragonite to calcite under fluid-buffered conditions. Thus, changes in relative sea level could in fact account for much of the variability in the Neogene marine $\delta^{13}C$ record.

CHC stromatolites are comprised of primary calcite microlaminae in association with secondary sparite outside the mat. Early diagenetic transformation of metastable carbonate phases to more stable calcite could bias the carbon isotope signature preserved in these samples if the process occurred under fluid-buffered versus sediment-buffered conditions. Carbon is typically assumed to be robust to diagenetic alteration due to sediment buffering of a carbonate-rich system. This contrasts with oxygen, which is more likely to be fluid buffered due to the relative abundance of water during diagenesis. High burial temperatures could result in significant degradation of sedimentary organic matter associated with thermal cracking and shift the DIC pool closer to organic-derived carbon sources. Carbonate $\delta^{13}C$ and $\delta^{18}O$ values for CHC mat calcite and secondary sparite are similar despite different modes and timescales of genesis, with no consistent relationship between Δ_{47}, $\delta^{13}C$ and $\delta^{18}O$ data. While one cannot exclude fluid-buffering of the carbon pool during any transformation of metastable mat carbonate to calcite, it is assumed here that mats represent primary or sediment-buffered conditions for carbon and either sediment-buffered or fluid-buffered system for oxygen.

Due to the 1.1 Ga age of the CHC, Δ_{47} values of non-recrystallized primary carbonate most likely represent a mixed primary and secondary signature. Processes of non-equilibrium kinetic isotope fractionation and diagenetic alteration of primary carbonate after formation are all expected to yield temperatures higher than conditions during formation, as there is no convincing mechanism for producing colder temperatures via secondary processes after burial. Thus, while other geochemical studies such as magnetic susceptibility (Petryshyn *et al.*, 2016) could potentially provide additional constraints on the extent of possible diagenetic alteration of primary carbonate for the CHC mats, it is believed that the low temperatures preserved in stromatolitic carbonate record maximum crystallization temperature at or soon after

formation. There is no simple scenario to explain the generation of cooler Δ_{47} temperatures due to burial for a billion years and briefly, at temperatures up to 125°C. Thermal history modelling of the MCR indicates that for a carbonate formed at 25°C, temperatures >140°C would be required to alter clumped isotope temperatures by more than +10°C, with no increase in apparent clumped temperature for burial at 125°C (Gallagher *et al.*, 2017). Thus, because the maximum alteration temperatures were at or below that threshold, Δ_{47} data could provide a maximum T °C of the palaeoenvironment but no information on whether or not conditions were significantly cooler than this. These data do indicate, however, that the mat carbonates did not experience enough heating to fully reset clumped isotope data.

Despite uncertainty in the absolute temperature of formation, Δ_{47} data record a maximum formation temperature of less than 30°C. The low temperatures recorded by stromatolite carbonate within the CHC as well as associated sparite suggests that organic carbon occluded within these same layers also likely did not experience significant thermal degradation or recrystallization associated with higher burial temperatures. Significant alteration of kerogen $\delta^{13}C$ values only occurs at much higher temperatures (>500°C; Peters *et al.*, 1981; Schoell, 1984), and abiogenic generation of isotopically depleted values requires both high temperature and high pressure (McCollom and Seewald, 2006). Based on this, it is assumed that neither carbonate nor organic matter carbon isotopic compositions are likely to have been altered dramatically from primary compositions.

5.2 | Stromatolite Organic Matter, Carbon isotopes and Implications for Mesoproterozoic pCO_2

A number of authors have used organic $\delta^{13}C$ data to quantify the concentration of DIC (Eichmann and Schidlowski, 1975; Popp *et al.*, 1989), most commonly with free-floating aquatic organisms that can take up aqueous CO_2 directly from the surrounding water. This approach is founded on the observation that autotrophic photosynthetic carbon fixation involves transport of inorganic carbon to the site of fixation and binding with the C-fixing enzyme (O'Leary, 1981; Farquhar *et al.*, 1982). In aqueous environments and for organisms without active CO_2 transport, the $\delta^{13}C$ of fixed carbon is controlled by the rate of diffusion of CO_2 to the fixation site and the isotopic composition of the dissolved $CO_{2(aq)}$ pool. The overall isotope effect can be described by:

$$\varepsilon_p = \varepsilon_t + \left(\varepsilon_f - \varepsilon_t\right) p_i/p_a \quad (1)$$

where ε_p equals the isotope effect associated with C fixation, ε_t = fractionation associated with CO_2 diffusion ($\varepsilon_{tw} = -0.7‰$ in water), ε_f = isotopic fractionation associated with C fixation by the Rubisco enzyme (~−29‰) and p_i and p_a reflect the internal and ambient pCO_2 (O'Leary, 1981; Farquhar *et al.*, 1982; Popp *et al.*, 1989). Such an approach provides a reasonable estimate of the effect of carbon limitation (i.e. concentration) on isotope discrimination.

In an aqueous system, the isotope effect can be described by $\varepsilon_p = ([\delta_p + 1{,}000)/(\delta_d + 1{,}000] - 1)$ 1,000 where δ_p represents organic fixed carbon and δ_d the DIC. The $\delta^{13}C_{aq}$ is recorded by $\delta^{13}C_{carb}$, and follows the temperature-dependent fractionation between DIC and calcite (Deines *et al.*, 1974). The $\delta^{13}C_{org}$ represents δ_p and is paired with $\delta^{13}C_{DIC}$ to quantify carbon isotope discrimination during biosynthetic C fixation. Inorganic carbonate $\delta^{13}C$ may be related to $\delta^{13}C_{CO_{2aq}}$ using the temperature-dependent fractionation between $CO_{2(g)}$ and $CO_{2(aq)}$ (Deines *et al.*, 1974).

The CHC microbial mats were formed in a braidplain system (Elmore, 1983, 1984; Sheldon, 2012; Wilmeth *et al.*, 2014; Petryshyn *et al.*, 2015; Fedorchuk *et al.*, 2016) and preserve ancient organic carbon, as well as mat-associated carbonate. As a result, these systems record the isotopic composition of fixed organic carbon and the DIC that may have been utilized for C fixation during growth in these systems. Microbial mats present a more complex system with respect to carbon cycling/diffusion than individual free-floating cellular organisms, yet the fundamental principles of carbon discrimination remain unchanged. Mats can be treated effectively as an ecosystem that ultimately is limited by the same factors (carbon, major and minor nutrients, nitrogen and available chemical or light energy) as a single cell. Mat organic carbon and carbonate $\delta^{13}C$ are used to provide bounds on carbon discrimination during mat formation that can be related to general carbon limitation. For photoautotrophs, this is ultimately limited by the DIC pool, which in many cases is controlled by atmospheric pCO_2. The $\delta^{13}C_{calcite}$ is used to constrain $\delta^{13}C_{aq}$ following Deines *et al.* (1974) using an assumed temperature of 25 and 40°C. These temperatures are consistent with surface conditions proposed by Fiorella and Sheldon (2017) for these palaeolatitudes under a variety of greenhouse gas scenarios, as a plausible but poorly constrained palaeotemperature. Reconstructed clumped isotope temperatures from the CHC stromatolites of 22–44°C provide some additional support for this range of potential mat environmental conditions. Mean $\delta^{13}C_{aq}$ values range from −10.8 at 25°C to −9.6‰ at 40°C (Table 3). Combined with mean organic carbon $\delta^{13}C$ of stromatolite laminae (−25.8‰), these data yield calculated ε_p values of 15.4–16.7. If the most depleted organic carbon isotope values represent the primary $\delta^{13}C_{org}$, absolute ε_p values for CHC mats range from 17.1 to 18.4.

Stromatolite carbon isotopes and ε_p can be related to DIC concentrations and ultimately ambient CO_2 if (a) the mechanisms of carbon fixation/mat formation are known and (b) modern isotope systematics show a relationship to ambient

CO_2 in the environment of formation. A variety of mechanisms drive the formation of carbonate within stromatolitic mats (Dupraz *et al.*, 2009), including uptake of CO_2 during photosynthesis and degassing of CO_2 from waters. Depending on the formation environment, aqueous systems may be in varied states of CO_2 disequilibrium relative to the atmosphere. The CHC mats are draped over large cobbles, formed on conglomeratic lenses and infilled with sands, gravels and silts associated with the alluvial fan of the Mesoproterozoic Rift (Figure 2). Associated with these stromatolites are intact mud-cracks and ripples, some containing gypsum, as well as recognized exposure surfaces (Elmore, 1983, 1984) that indicate a shallow, episodically sub-aerial and variable-energy aqueous system. CHC mats were formed in shallow water, within the photic zone. In addition, acritarchs found in associated sediments (Wellman and Strother, 2015) and carbon isotopes of organic matter within the CHC mats and penecontemporaneous floodplain mats (Sheldon, 2012) strongly suggest phototrophy as a key metabolism. Thus, it is highly probably that CHC mat carbon fixation was underpinned by phototrophic metabolism. Growth waters were likely at least somewhat mixed with respect to the atmosphere. Environments characterized by high shear stress have potential to inhibit microbial mat accumulation; thus, mat structures preserved in the CHC could have formed during intervals of greater quiescence within an otherwise turbid system (Elmore, 1983). Such conditions would be more prone to restriction, with mat accumulation representative of low energy intervals. However, regular intermixing of coarse sand and sediment as well as large cobbles within mat layers indicates that the frequent intervals of turbidity were likely a regular feature of the system (Figure 2C). Furthermore, direct association of mats with ripples strongly support growth in an environment with moving water that is likely to have greater exchange of dissolved gases between the aqueous environment and the atmosphere.

The second condition that must be met to relate mat carbon isotopes to ambient CO_2 is that modern mats must show a relationship between DIC, pCO_2 and carbon discrimination. Chemostat experiments show that ε_p of photosynthetic autotrophs is controlled by dissolved CO_2, nutrient availability, growth rate and, for single cells, cellular volume to surface

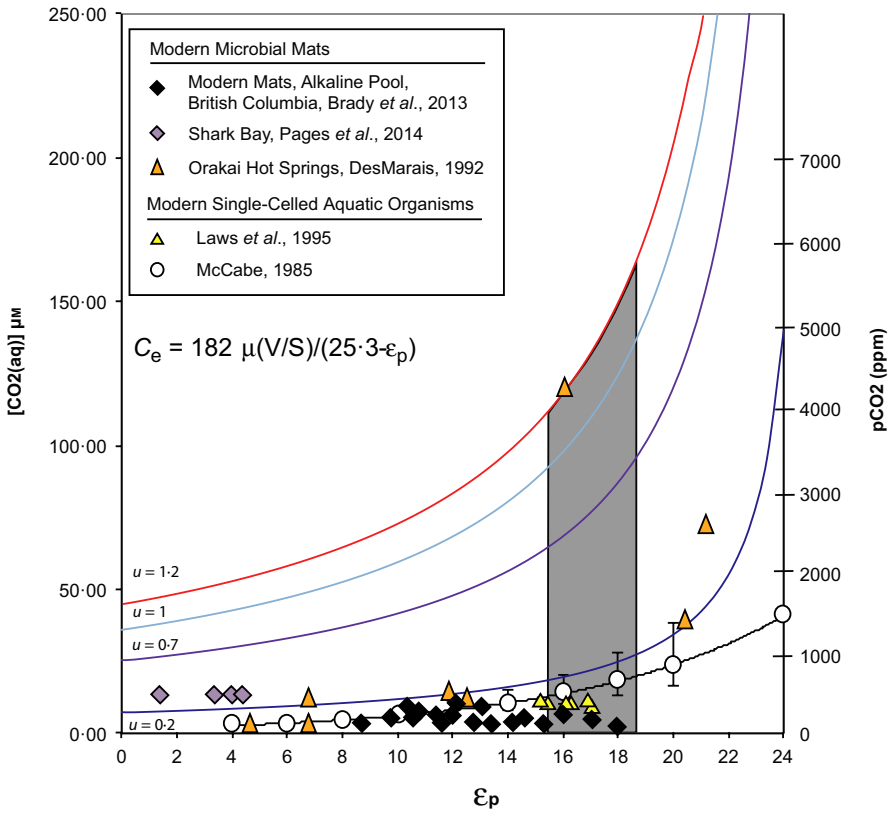

FIGURE 4 Carbon isotope discrimination (ε_p) between mat organic matter and $CO_{2(aq)}$ for modern microbial mats from alkaline, evaporative marine and hydrothermal systems. For reference, ε_p data and predictions for single-celled aquatic organisms as a function of $CO_{2(aq)}$ are shown. Solid lines represent the empirically derived relationships between C isotope discrimination and $CO_{2(aq)}$ for single-celled organisms with a volume to surface area (V/S) ratio of 5 and varied growth rates (μ/d) after Laws *et al.* (1995). Gray shaded area shows the calculated ε_p values for CHC mats. The CHC mats yield ε_p values compatible with modern mats in waters with low $CO_{2(aq)}$, and fall below the empirical relationship for slow-growing photoautotrophs ($\mu = 0.2$) with moderate to high V/S ratios. The ε_p data are compatible with mats formed in waters with $CO_{2(aq)}$ that is equivalent to less than ~20 PAL, and most consistent with Mesoproterozoic pCO_2 of less than several times PAL

area ratio (V/S) (Popp *et al.*, 1989; Laws *et al.*, 1995; Dupraz *et al.*, 2009) (Figure 4). In a well-mixed water body, the $\delta^{13}C_{org}$ of individual aquatic photosynthesizers reflects isotopic discrimination associated with diffusion of CO_2 to the site of C fixation and the dissolved CO_2 is proportional to atmospheric pCO_2. In biogenic stromatolitic mats, fine-scale carbon isotope systematics are highly variable with depth in the mat due to unique assemblages of symbiotic organisms and restrictions on gas diffusion through the mat. Despite these complexities, empirical data show that just as for free-floating aquatic organisms, the amount of dissolved CO_2 in water is generally the first-order C limitation for photoautotrophs within a mat. This limitation is in part recorded in the biomass $\delta^{13}C$ of mat ecosystems, which integrate material from chemoautotrophs or photoautotrophs and the heterotrophs that feed on them or their exudates. As with single-celled organisms, modern empirical data show that bulk mat ε_p approaches a maxima when pCO_2 or dissolved CO_2 is high in the aqueous environment (Figure 4). This empirical observation provides an important, if imperfect tool to assess past pCO_2, particularly when estimates for atmospheric pCO_2 range from several times PAL to >100 PAL.

Studies of carbon isotope fractionation during CO_2 uptake and photosynthetic fixation show a strong dependence on dissolved aqueous CO_2 concentration (Popp *et al.*, 1989). Under conditions of low CO_{2aq} and pCO_{2atm}, $\delta^{13}C$ of organic biomass shows significantly reduced carbon isotope discrimination, while under high CO_2 availability, carbon isotope discrimination approaches a theoretical maximum (Popp *et al.*, 1989). Data from modern microbial mat carbonates formed in marine hypersaline, freshwater alkaline and hydrothermal systems were used to calculate carbonate isotope discrimination () as a function of variable [DIC] using published $\delta^{13}C_{carbonate}$, $\delta^{13}C_{mat}$ and DIC data (Des Marais *et al.*, 1992; Brady *et al.*, 2013; Pagès *et al.*, 2014). The value is calculated after Laws *et al.* (1995), where $\varepsilon = (1{,}000\ (\delta^{13}C_{org} - \delta^{13}C_{aq})/(1{,}000 + \delta^{13}C_{org}))$. For clarification, the $\delta^{13}C$ of organic matter was compared relative to $\delta^{13}C_{aq}$ (not $\delta^{13}C_{DIC}$) to quantify ε. The $\delta^{13}C_{gas}$ was calculated from the isotopic composition of associated carbonates using the empirical $\delta^{13}C_{carb}/\delta^{13}C_{aq}$ fractionation factor determined by Deines *et al.* (1974). Figure 4 shows measured ε versus CO_{2aq} for modern microbial mats in alkaline pools in British Columbia (Brady *et al.*, 2013), Orakei Hot Springs (Des Marais *et al.*, 1992) and Shark Bay (Pagès *et al.*, 2014), as well as data for free-floating single cell growth experiments (McCabe, 1985; Laws *et al.*, 1995), and the pCO_2 that would be calculated for an atmosphere in equilibrium with the dissolved CO_{2aq}. These data provide boundary conditions for examining the isotopic values recorded by CHC mat carbonate and organic matter. The pCO_2 values associated with each ε value for modern mats do not represent true atmospheric pCO_2, but rather the calculated pCO_2 based on the measured dissolved CO_2 concentration (DIC in μmol/l), water temperature, Henry's constant for CO_2 and assumption of equilibrium between DIC and the atmosphere. Using this approach, the calculated atmospheric pCO_2 for waters associated with carbonate-bearing microbial mats in British Columbia (Brady *et al.*, 2013) ranges from 93 to 413 ppm with a mean of 208 ppm. Modern data for Orakei hot springs have high DIC and high CO_{2aq} and are not in equilibrium with the atmosphere due to high dissolved CO_2. These produce a theoretical pCO_{2atm} value significantly in excess of modern and are included to demonstrate that waters in equilibrium with far higher dissolved CO_2 concentrations than the modern still follow the general patterns of carbon isotope discrimination observed in other mat systems. The modern mat C data shown here are derived from environments with flowing water, lakes and marine systems, with mixed microbial communities. All follow the general relationship between [DIC] and carbon isotope discrimination within the mat.

Modern mats exhibit smaller ε_p than plants or single-celled photoautotrophs for comparable pCO_2, likely due to diffusion limitation at the water–mat interface, C-limited cellular growth rates and recycling of C within the mat system. The difference is greatest in modern mats in hypersaline or high temperature conditions where ε_p values may range from ~1 to 14 for a range of dissolved aqueous CO_2. Stromatolitic mats today are characterized by complex cycling of carbon that varies as a function of microbial assemblages and aqueous conditions. Thus, it is known that there can be significant variation in CO_{2aq} and $\delta^{13}C_{org}$ within a mat and between different mat types (Dupraz *et al.*, 2009). This heterogeneity was likely no different in the deep past. For example, Lepot *et al.* (2009) show large variability in $\delta^{13}C$ of organic matter in 2.72 Ga microbial structures, highlighting the role of microbial metabolism in controlling isotope heterogeneity on the micron scale and larger. Despite this, microbial mats are ecosystems comprised of an array of communities assembled into effectively a single structure. All organisms within this system are ultimately limited by one or more nutrients, including carbon. From an ecosystem perspective, modern data provide semi-quantitative boundary conditions for interpreting ancient mat systems, particularly when considering ancient systems for which some suggest pCO_2 was in excess of 30–100 PAL. Modern data demonstrate that for most shallow mat systems within the photic zone with a significant proportion of phototrophs, mats as a whole are sensitive to large changes in CO_{2aq}, producing a large increase in ε for only modest increases in CO_{2aq}. A mat within a mixed aquatic system can effectively be thought of as a system with a very large volume to surface area ratio (surface area being the exposed interface between the mat and ambient water), whereas under quieter conditions, effective volume to surface area would be lower. Modern mat isotope data match reasonably well (Figure 4) with CO_2-carbon isotope sensitivity observed

in modern free-floating low volume to surface area microbes with slow growth rate (McCabe, 1985; Laws *et al.*, 1995).

One potential complication to the approach used here to constrain past DIC and ultimately pCO_2, is if CO_2 was not the primary C source supporting the mat system. For example, Olsen *et al.* (2016) suggest that marine methanotrophy coupled with sulphate reduction could have been an important component of C and S cycling in the Mesoproterozoic, serving as a limit to buildup of CH_4 in the atmosphere. If the mat ecosystem was dominated by methanotrophy with CH_4 available via sources outside the mat, this would render expected relationships between mat $\delta^{13}C$ and atmospheric pCO_2 (by virtue of the relationship with DIC) void. Methanotrophs can derive energy via either anaerobic or aerobic pathways. In the modern, mats underpinned by anaerobic methanotrophy are observed in areas of methane and other hydrocarbon seeps and often associated with sulphate reduction (Drake *et al.*, 2015). In benthic mats near seeps, methanotrophy may contribute nearly 50% of total fatty acids in mat organics (Ding and Valentine, 2008). However, CHC mats are located in a relatively shallow ancient braidplain and are associated with mud-cracks and gypsum, indicating at least somewhat oxic conditions and free sulphate at or around the time of mat formation. In addition, anaerobic methanotrophy is known to generate some of the most depleted $\delta^{13}C$ values in carbonate (−125‰; Drake *et al.*, 2015). While it is impossible to rule out methanotrophy as an important metabolism within CHC mats, fossil evidence of phototrophs and $\delta^{13}C$ data are consistent with phototrophy.

Carbonate and organic $\delta^{13}C$ data from CHC stromatolites are coupled with clumped isotope temperatures to provide reasonable boundary conditions for $\delta^{13}C_{CO_{2aq}}$, ε_p and CO_{2aq}. Because mat samples derive from a system with at least intermittently moving water (Figure 2) and underlain by non-carbonate bedrock, it is assumed that limitation to CO_2 diffusion into or out of the water system is far less than within the mat system. Thus, even in slow or occasionally stagnant water, CO_2 diffusion into the mat is likely the primary limitation to carbon assimilation within the mat as a whole. With these assumptions, modern data provide reasonable, if imprecise limits for interpreting palaeo-ε data with respect to ancient CO_{2aq} and pCO_2 within the palaeoenvironment. Specifically, carbon discrimination data from modern hot springs are used as an upper limit for ε_p–pCO_2 relationships in the ancient. Measured ε_p values for the Proterozoic stromatolites range from 15.4 to 18.4 for temperatures of 25–40°C. Modern mat ε_p values are all less than 21‰ and mats that record an ε_p of less than 18‰ are found in waters in equilibrium with DIC of less than 130 μM, consistent with a pCO_2 effectively less than 1,000 ppm. Modern mat carbon discrimination data generally follow the pattern of ε_p versus DIC observed in slow growing cells with moderate to high volume to surface area (Figure 4). The ε_p data for CHC mats are equivalent to modern mats grown in waters with DIC and in theoretical equilibrium with pCO_2 of less than ~20 PAL, and most consistent with mat data for waters in equilibrium with pCO_2 of less than several times PAL. While pCO_2 estimates based on $\delta^{13}C_{org}$–$\delta^{13}C_{DIC}$ require accurate measurement of primary $\delta^{13}C_p$ and $\delta^{13}C_{aq}$ and optimally, equilibrium between the DIC and the atmosphere, these limits are consistent with palaeosol (Sheldon, 2006, 2013), single organism carbon discrimination (Kaufman and Xiao, 2003) and fossil carbonate-based (Bartley and Kah, 2004; Kah and Riding, 2007) estimates for late Mesoproterozoic pCO_2 (Figure 5). Thus, CHC stromatolite data are consistent with both temperate palaeoenvironmental conditions and relatively low pCO_2.

5.3 | Comparison of Temperature, pCO_2 and Mesoproterozoic AOGCMs

Reconstructions of the past solar insolation indicate that a 'faint young Sun' paradox exists throughout the Precambrian wherein equable conditions would need to have been maintained in the presence of significantly lower insolation that has increased steadily from less than 70% of the present day value over the past 4.5 Ga (Gough, 1981). Recent work by Fiorella and Sheldon (2017) using 91% total solar insolation (Gough, 1981) shows that an equable Mesoproterozoic climate could have been maintained by increased CH_4 flux from methanogenic bacteria even in the absence of strongly elevated pCO_2. The AOGCM outputs show that ice-free conditions could be maintained for $pCO_2 < 10$ PAL with the threshold for regional-scale glaciation occurring with CH_4 at 28 ppmv or pCO_2 below 5 PAL. These results are in agreement with temperatures for ~30° latitude predicted by AOGCM simulations of the Mesoproterozoic using these boundary conditions (Figure 6). Recent work by Olson *et al.* (2016) suggests that anaerobic oxidation of CH_4 coupled with SO_4^{2-} reduction could act as an obstacle to CH_4 accumulation in the atmosphere, limiting pCH_4 to less than 10 ppmv if the only source of CH_4 is marine production, independent of pO_2. If both the AOGCM results (Fiorella and Sheldon, 2017) and modelled CH_4 fluxes are correct (Daines and Lenton, 2016; Olson *et al.*, 2016), a paradox develops because the apparent CH_4 level would be too low to support the observed equable conditions.

There are at least two potential solutions to this paradox. The first is that a marine-only model of CH_4 flux underestimates the total biogenic CH_4 flux. As noted above, there is extensive evidence for a significant lake and floodplain biosphere (Elmore, 1983; Sheldon, 2012; Wellman and Strother, 2015) by the Mesoproterozoic and many stable isotopic values from those systems, especially in palaeo-lake sediments (Imbus *et al.*, 1992), are too negative to have been the result of C derived only from photosynthetic means. Thus, a potentially large terrestrial biogenic CH_4 flux is supported by existing

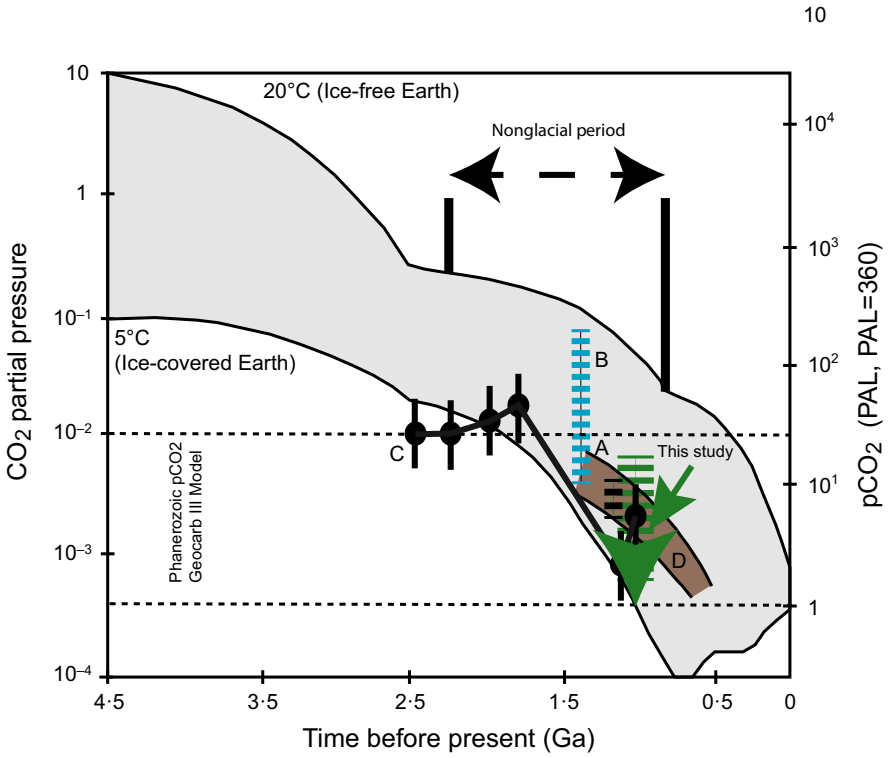

FIGURE 5 Proterozoic pCO_2 ranges. Gray shaded area shows upper and lower pCO_2 limits for an ice-free (20°C) and glacial (5°C) world based on photochemical model estimates (Kasting, 1987). Calculated pCO_2 estimates (<20 PAL and most likely <5 PAL) agree with (A) cyanobacterial calcification (Kah and Riding, 2007), (B) minimum isotopic (Kaufman and Xiao, 2003), (C) palaeosol mass balance (Sheldon, 2006, 2013; Mitchell and Sheldon, 2010) and (D) carbon reservoir modelling (Bartley and Kah, 2004) estimates. These data support equable Mesoproterozoic temperatures and low pCO_2. These data indicate that CH_4 or some other greenhouse gas (e.g. N_2O) likely played a role in regulating global temperature and provided a negative feedback to the buildup of atmospheric oxygen (figure modified from Kah and Riding, 2007)

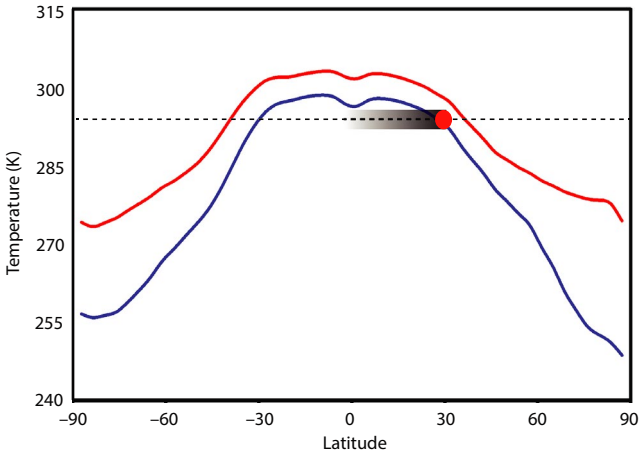

FIGURE 6 Calculated zonal mean temperatures for the Mesoproterozoic using boundary conditions of 5 PAL CO_2 (bottom line) and 10 PAL and 140 ppm CH_4 (top line) and Mesoproterozoic palaeogeography (Fiorella and Sheldon, 2017). Upper boundary for Mean Annual Air Temperature (MAAT) for the tropics and/or near tropical regions (<30° latitude) is shown (circle and shaded area) based on stromatolite Δ_{47} temperature data that may reflect a combination of primary and/or early diagenetic alteration of original clumped isotope signatures

constraints. This idea was recently tested by Zhao *et al.* (2017) who modelled the potential for a significant terrestrial CH_4 flux to supplement the marine CH_4 flux. They found that if terrestrial cyanobacterial mats covered 8%–10% of the Earth's surface, clement conditions would have been maintained even at the relatively low pCO_2 values indicated by palaeosols (Sheldon, 2013) and, as reported herein, microbialites.

Secondly, atmospheric model simulations have typically focused on a narrow range of greenhouse gases that include CO_2, CH_4 and sometimes H_2O vapour (cf. Roberson *et al.*, 2011). However, there are a number of other greenhouse gases that have significantly higher climate forcings than CO_2 that are poorly constrained in the geologic record. For example, as Fiorella and Sheldon (2017) noted, one potential way to reconcile differences in CH_4 levels is with N_2O (e.g. see Roberson *et al.*, 2011). While there are no direct proxies for pN_2O, a 10-fold increase from the modern value of 0.3 ppm would provide enough additional greenhouse forcing to offset a fivefold lower pCH_4 value. Thus, there are at least two potential solutions to the apparent CH_4 paradox that would bear further investigation. Ultimately, the development of proxies for greenhouse gases beyond CO_2 would substantially enhance our ability to reconcile the challenges presented by the 'faint young Sun' paradox across the whole of the Precambrian.

6 | CONCLUSIONS

Sedimentary features and organic and inorganic carbon isotope data from 1.1 Ga stromatolites in the CHC indicate formation in waters with relatively low DIC. This most likely results from equilibrium with a relatively low atmospheric pCO_2 (less than 20 PAL; Figures 4 and 5) during a time when solar luminosity was ~9% lower than today. If pCO_2 was indeed lower than this bound, elevated concentrations of other greenhouse gases, such as methane, may have played a role in regulating global temperature. However, current estimates of the potential Mesoproterozoic CH_4 flux from marine environments are relatively low, creating a methane paradox. The paradox is potentially resolvable either through a relatively extensive terrestrial biosphere or through elevated levels of other greenhouse gases such as N_2O. At present, the means to test between those hypotheses is lacking, but if biologically produced gases such as CH_4 played a key role in regulating global temperature during the Mesoproterozoic, their concentrations may have acted as a negative feedback to the buildup of atmospheric O_2 due to the potential to oxidize readily in the presence of free oxygen as well as providing global climate regulation.

ACKNOWLEDGEMENTS

This work was supported in part by the University of Michigan Turner Postdoctoral Fellowship funding to M.T.H. and NSF EAR 1050760 to N.D.S.

CONFLICT OF INTEREST

The authors certify that they have no affiliations with or involvement in any organization or entity with any financial interest, or non-financial interest in the subject matter or materials discussed in this manuscript.

DATA AVAILABILITY STATEMENT

The authors confirm that the data supporting the findings of this study are available within the article and its supplementary materials.

REFERENCES

Affek, H.P., Bar-Matthews, M., Ayalon, A., Matthews, A. and Eiler, J.M. (2008) Glacial/interglacial temperature variations in Soreq cave speleothems as recorded by "clumped isotope" thermometry. *Geochimica et Cosmochimica Acta*, *72*, 5351–5360.

Ahm, A.-S.C., Bjerrum, C.J., Swart, P.K. and Higgins, J.A. (2018) Quantifying early marine diagenesis in shallow-water carbonate sediments. *Geochimica et Cosmochimica Acta*, *236*, 140–159.

Bartley, J.K. and Kah, L.C. (2004) Marine carbon reservoir, C_{org}-C_{carb} coupling, and the evolution of the Proterozoic carbon cycle. *Geology*, *32*, 129–132.

Beghin, J., Storme, J.-Y., Blanpied, C., Gueneli, N., Brocks, J.J., Poulton, S.W. et al. (2017) Micro fossils from the late Mesoproterozoic-early Neoproterozoic Atar/El Mreiti Group, Taoudeni Basin, Mauritania, northwestern Africa. *Precambrian Research*, *291*, 63–82.

Bernasconi, S.M., Müller, I.A., Bergmann, K.D., Breitenbach, S.F.M., Fernandez, A., Hodell, D.A. et al. (2018) Reducing uncertainties in carbonate clumped isotope analysis through consistent carbonate-based standardization. *Geochemistry, Geophysics, Geosystems*, *19*, 2895–2914.

Brady, A.L., Druschel, G., Leoni, L., Lim, D. and Slater, G.F. (2013) Isotopic biosignatures in carbonate-rich, cyanobacteria-dominated microbial mats of the Cariboo Plateau, BC. *Geobiology*, *11*, 437–456.

Cannon, W.F. and Hinze, W.J. (1992) Speculations on the origin of the North American Midcontinent rift. *Tectonophysics*, *213*, 49–55.

Cumming, V.M., Poulton, S.W., Rooney, A.D. and Selby, D. (2013) Anoxia in the terrestrial environment during the late Mesoproterozoic. *Geology*, *41*, 583–586.

Daëron, M., Guo, W., Eiler, J., Genty, D., Blamart, D., Boch, R., et al. (2011) 13C18O clumping in speleothems: observations from natural caves and precipitation experiments. *Geochimica et Cosmochimica Acta*, *75*, 3303–3317.

Daines, S.J. and Lenton, T.M. (2016) The effect of widespread early aerobic marine ecosystems on methane cycling and the Great Oxidation. *Earth and Planetary Science Letters*, *434*, 42–51.

Davis, D.W. and Paces, J.B. (1990) Time resolution of geologic events on the Keweenaw Peninsula and implications for development of the Midcontinent Rift system. *Earth and Planetary Science Letters*, *97*, 54–64.

Defliese, W.F., Hren, M.T. and Lohmann, K.C. (2015) Compositional and temperature effects of phosphoric acid fractionation on Δ47 analysis and implications for discrepant calibrations. *Chemical Geology*, *396*, 51–60.

Deines, P., Langmuir, D. and Harmon, R.S. (1974) Stable carbon isotope ratios and the existence of a gas phase in the evolution of carbonate ground waters. *Geochimica et Cosmochimica Acta*, *38*, 1147–1164.

Dennis, K.J., Affek, H.P., Passey, B.H., Schrag, D.P. and Eiler, J.M. (2011) Defining an absolute reference frame for "clumped" isotope studies of CO_2. *Geochimica et Cosmochimica Acta*, *75*, 7117–7131.

Des Marais, D.J., Bauld, J., Palmisano, A.C., Summons, R.E. and Ward, D.M. (1992) The biogeochemistry of carbon in modern microbial mats. In J. William Schopf & C. Klein *The Proterozoic Biosphere: A Multidisciplinary Study*. Cambridge: Cambridge University Press, pp. 299–308.

Ding, H., & Valentine, D.L. (2008). Methanotrophic bacteria occupy benthic microbial mats in shallow marine hydrocarbon seeps, Coal Oil Point. *California. J. Geophys. Res.*, *113*, G01015.

Douglas Elmore, R., Milavec, G.J., Imbus, S.W. and Engel, M.H. (1989) The Precambrian nonesuch formation of the North American midcontinent rift, sedimentology and organic geochemical aspects of lacustrine deposition. *Precambrian Research*, *43*, 191–213.

Drake, H., Åström, M.E., Heim, C., Broman, C., Åström, J., Whitehouse, M. *et al*. (2015). Extreme (13)C depletion of carbonates formed during oxidation of biogenic methane in fractured granite. *Nature Communications*, *6*, 7020.

Dupraz, C., Reid, R.P., Braissant, O., Decho, A.W., Norman, R.S. and Visscher, P.T. (2009) Processes of carbonate precipitation in modern microbial mats. *Earth Science Reviews*, *96*, 141–162.

Eagle, R.A., Eiler, J.M., Tripati, A.K., Ries, J.B., Freitas, P.S., Hiebenthal, C., et al. (2013) The influence of temperature and seawater carbonate saturation state on ^{13}C–^{18}O bond ordering in bivalve mollusks. *Biogeosciences*, *10*, 4591–4606.

Eichmann, R. and Schidlowski, M. (1975) Isotopic fractionation between coexisting organic carbon—Carbonate pairs in Precambrian sediments. *Geochimica et Cosmochimica Acta*, *39*, 585–595.

Elmore, R.D. (1983) Precambrian non-marine stromatolites in alluvial fan deposits, the Copper Harbor Conglomerate, upper Michigan. *Sedimentology*, *30*, 829–842.

Elmore, R.D. (1984) The copper harbor conglomerate: a late Precambrian fining-upward alluvial fan sequence in northern Michigan. *Geological Society of America Bulletin*, *95*, 610–617.

Farquhar, G.D., O'Leary, M.H. and Berry, J.A. (1982) On the relationship between carbon isotope discrimination and the intercellular carbon dioxide concentration in leaves. *Functional Plant Biology*, *9*, 121–137.

Fedorchuk, N.D., Dornbos, S.Q., Corsetti, F.A., Isbell, J.L., Petryshyn, V.A., Bowles, J.A. et al. (2016) Early non-marine life: evaluating the biogenicity of Mesoproterozoic fluvial-lacustrine stromatolites. *Precambrian Research*, *275*, 105–118.

Fiorella, R.P. and Sheldon, N.D. (2017) Equable end Mesoproterozoic climate in the absence of high CO_2. *Geology*, *45*(3), 231–234. https ://doi.org/10.1130/G38682.1

Frantz, C.M., Petryshyn, V.A., Marenco, P.J., Tripati, A., Berelson, W.M. and Corsetti, F.A. (2014) Dramatic local environmental change during the Early Eocene Climatic Optimum detected using high resolution chemical analyses of Green River Formation stromatolites. *Palaeogeography, Palaeoclimatology, Palaeoecology*, *405*, 1–15.

Gallagher, T.M., Sheldon, N.D., Mauk, J.L., Petersen, S.V., Gueneli, N. and Brocks, J.J. (2017) Constraining the thermal history of the North American Midcontinent Rift System using carbonate clumped isotopes and organic thermal maturity indices. *Precambrian Research*, *294*, 53–66.

Ghosh, P., Adkins, J., Affek, H., Balta, B., Guo, W., Schauble, E.A. *et al*. (2006). 13 C–18 O bonds in carbonate minerals: A new kind of paleothermometer. *Geochimica et Cosmochimica Acta*, *70*(6), 1439–1456.

Gough, D.O. (1981) Solar interior structure and luminosity variations. *Solar Physics*, *74*, 21–34.

Henkes, G.A., Passey, B.H., Grossman, E.L., Shenton, B.J., Pérez-Huerta, A. and Yancey, T.E. (2014) Temperature limits for preservation of primary calcite clumped isotope paleotemperatures. *Geochimica et Cosmochimica Acta*, *139*, 362–382.

Higgins, J.A., Blättler, C.L., Lundstrom, E.A., Santiago-Ramos, D.P., Akhtar, A.A., Crüger, Ahm A.S., et al. (2018) Mineralogy, early marine diagenesis, and the chemistry of shallow-water carbonates. *Geochimica et Cosmochimica Acta*, *220*, 512–534.

Hren, M.T. and Sheldon, N.D. (2012) Temporal variations in lake water temperature: paleoenvironmental implications of lake carbonate $\delta^{18}O$ and temperature records. *Earth and Planetary Science Letters*, *337–338*, 77–84.

Hutchinson, D.R., White, R.S., Cannon, W.F. and Schulz, K.J. (1990) Keweenaw hot spot: geophysical evidence for a 1.1 Ga mantle plume beneath the Midcontinent Rift System. *Journal of Geophysical Research*, *95*, 10869–10884.

Imbus, S.W., Macko, S.A., Elmore, R.D., & Engel, M.H. (1992). Stable isotope (C, S, N) and molecular studies on the Precambrian Nonesuch Shale (Wisconsin-Michigan, USA): evidence for differential preservation rates, depositional environment and hydrothermal influence. *Chemical Geology: Isotope Geoscience Section*, *101*(3–4), 255–281.

Kah, L.C. and Riding, R. (2007) Mesoproterozoic carbon dioxide levels inferred from calcified cyanobacteria. *Geology*, *35*, 799–802.

Kanzaki, Y., & Murakami, T. (2015). Estimates of atmospheric CO2 in the Neoarchean–Paleoproterozoic from paleosols. *Geochimica et Cosmochimica Acta*, *159*, 190–219.

Kasting, J.F. (1987). Theoretical constraints on oxygen and carbon dioxide concentrations in the Precambrian atmosphere. *Precambrian Research*, *34*, 205–229.

Kaufman, A.J., & Xiao, S. (2003). High CO2 levels in the Proterozoic atmosphere estimated from analyses of individual microfossils. *Nature*, *425*(6955), 279–282.

Kah, L.C., Sherman, A.G., Narbonne, G.M., Knoll, A.H. and Kaufman, A.J. (1999) $\Delta^{13}C$ stratigraphy of the Proterozoic Bylot Supergroup, Baffin Island, Canada: implications for regional lithostratigraphic correlations. *Canadian Journal of Earth Sciences*, *36*, 313–332.

Kasting, J.F. (1993) Earth's early atmosphere. *Science*, *259*, 920–926.

Kaufman, A.J., Knoll, A.H., & Narbonne, G.M. (1997). Isotopes, ice ages, and terminal Proterozoic earth history. *Proceedings of the National Academy of Sciences of the United States of America*, *94*(13), 6600–6605.

Kaufman, A.J. and Xiao, S. (2003) High CO_2 levels in the Proterozoic atmosphere estimated from analyses of individual microfossils. *Nature*, *425*, 279–282.

Kennedy, M.J., Runnegar, B., Prave, A.R., Hoffmann, K.-H., & Arthur, M.A. (1998). Two or four Neoproterozoic glaciations? *Geology*, *26*(12), 1059–1063.

Kendall, B.S., Creaser, R.A., Ross, G.M., & Selby, D. (2004). Constraints on the timing of Marinoan "Snowball Earth" glaciation by 187 Re–187 Os dating of a Neoproterozoic, post-glacial black shale in Western Canada. *Earth and Planetary Science Letters*, *222*(3), 729–740.

Kim, S.-T., & O'Neil, J.R. (1997). Equilibrium and nonequilibrium oxygen isotope effects in synthetic carbonates. *Geochimica et Cosmochimica Acta*, *61*(16), 3461–3475.

Laws, E.A., Popp, B.N., Bidigare, R.R., Kennicutt, M.C. and Macko, S.A. (1995) Dependence of phytoplankton carbon isotopic composition on growth rate and (CO_2)aq: theoretical considerations and experimental results. *Geochimica et Cosmochimica Acta*, *59*, 1131–1138.

Lepot, K., Benzerara, K., Rividi, N., Cotte, M., Brown, G.E. and Philippot, P. (2009) Organic matter heterogeneities in 2.72 Ga stromatolites: alteration versus preservation by sulfur incorporation. *Geochimica et Cosmochimica Acta*, *73*, 6579–6599.

Livnat, A. (1983). *Metamorphism and copper mineralization of the Portage Lake Lava Series, northern*. Michigan (University of Michigan).

Lyons, T.W., Reinhard, C.T. and Planavsky, N.J. (2014) The rise of oxygen in Earth's early ocean and atmosphere. *Nature*, *506*, 307–315.

Mauk, J.L. and Hieshima, G.B. (1992) Geochemistry of Metalliferous Black Shales Organic matter and copper mineralization at White Pine, Michigan, U.S.A. *Chemical Geology*, *99*, 189–211.

McCabe, B. (1985) *The Dynamics of ^{13}C in Several New Zealand Lakes*. PhD Thesis, University of Waikato.

McCollom, T.M. and Seewald, J.S. (2006) Carbon isotope composition of organic compounds produced by abiotic synthesis under hydrothermal conditions. *Earth and Planetary Science letters*, *243*, 74–84.

Mitchell, R.L. and Sheldon, N.D. (2009) Weathering and paleosol formation in the 1.1 Ga Keweenawan Rift. *Precambrian Research*, *168*, 271–283.

Mitchell, R.L. and Sheldon, N.D. (2010) The ~1100 Ma Sturgeon Falls paleosol revisited: Implications for Mesoproterozoic weathering environments and atmospheric CO_2 levels. *Precambrian Research*, *183*, 738–748.

Mitchell, R.L. and Sheldon, N.D. (2016) Sedimentary provenance and weathering processes in the 1.1 Ga Midcontinental Rife of the Keweenaw Peninsula, Michigan, USA. *Precambrian Research*, *275*, 225–240.

Morey, G.B. and Ojakangas, R.W. (1982) 7D: Keweenawan sedimentary rocks of eastern Minnesota and northwestern Wisconsin. *Geological Society of America Memoirs*, *156*, 135–146.

Nishioka, G.K., Kelly, W.C. and Douglas Elmore, R. (1984) Copper occurrences in stromatolites of the Copper Harbor Conglomerate, Keweenaw Peninsula, northern Michigan. *Economic Geology*, *79*, 1393–1399.

Noffke, N. (2009) The criteria for the biogeneicity of microbially induced sedimentary structures (MISS) in Archean and younger, sandy deposits. *Earth Science Reviews*, *96*, 173–180.

Noffke, N. and Awramik, S.M. (2013) Stromatolites and MISS—differences between relatives. *GSA Today*, *23*, 4–9.

O'Leary, M.H. (1981) Carbon isotope fractionation in plants. *Phytochemistry*, *20*, 553–567.

Ohr, M. (1993) *Geochronology of diagenesis and low-grade metamorphism in pelites*. University of Michigan.

Olson, S.L., Reinhard, C.T. and Lyons, T.W. (2016) Limited role for methane in the mid-Proterozoic greenhouse. *Proceedings of the National Academy of Sciences of the USA*, *113*, 11447–11452.

Pagès, A., Grice, K., Ertefai, T., Skrzypek, G., Jahnert, R. and Greenwood, P. (2014) Organic geochemical studies of modern microbial mats from Shark Bay: part I: influence of depth and salinity on lipid biomarkers and their isotopic signatures. *Geobiology*, *12*, 469–487.

Parnell, J., Spinks, S., Andrews, S., Thayalan, W. and Bowden, S. (2015) High Molybdenum availability for evolution in a Mesoproterozoic lacustrine environment. *Nature Communications*, *6*, 6996.

Peters, K.E., Rohrback, B.G. and Kaplan, I.R. (1981) Carbon and hydrogen stable isotope variations in kerogen during laboratory-simulated thermal maturation. *AAPG Bulletin*, *65*, 501–508.

Peterson, S.V., Defliese, W.F., Saenger, C., Daëron, M., Huntington, K.W., John, C.M. et al. (2019) Effects of improved 17O correction on inter-laboratory agreement in clumped isotope calibrations, estimates of mineral-specific offsets, and temperature dependence of acid digestion fractionation. *Geochemistry, Geophysics, Geosystems*. https://doi.org/10.1029/2018gc008127

Petryshyn, V.A., Lim, D., Laval, B.L., Brady, A., Slater, G. and Tripati, A.K. (2015) Reconstruction of limnology and microbialite formation conditions from carbonate clumped isotope thermometry. *Geobiology*, *13*, 53–67.

Petryshyn, V.A., Corsetti, F.A., Frantz, C.M., Lund, S.P. and Berelson, W.M. (2016) Magnetic susceptibility as a biosignature in stromatolites. *Earth and Planetary Science Letters*, *437*, 66–75.

Planavsky, N.J., Reinhard, C.T., Wang, X., Thomson, D., McGoldrick, P., Rainbird, R.H., et al. (2014) Earth history. Low mid-Proterozoic atmospheric oxygen levels and the delayed rise of animals. *Science*, *346*, 635–638.

Planavsky, N.J., Cole, D.B., Isson, T.T., Reinhard, C.T., Crockford, P.W., et al. (2018) A case for low atmospheric oxygen levels during Earth's middle history. *Emerging Topics in Life Sciences*, *2*(2), 149–159. https://doi.org/10.1042/ETLS20170161

Popp, B.N., Takigiku, R., Hayes, J.M., Louda, J.W. and Baker, E.W. (1989) The post-Paleozoic chronology and mechanism of 13 C depletion in primary marine organic matter. *American Journal of Science*, *289*, 436–454.

Pratt, L.M., Summons, R.E. and Hieshima, G.B. (1991) Sterane and triterpane biomarkers in the Precambrian Nonesuch Formation, North American Midcontinent Rift. *Geochimica et Cosmochimica Acta*, *55*, 911–916.

Price, K.L., Huntoon, J.E. and McDowell, D.S. (1996) Thermal history of the 1.1-Ga Nonesuch Formation, North American Mid-continent Rift, White Pine, Michigan. *AAPG Bulletin*, *80*, 1–15.

Riding, R. (2011) The nature of stromatolites: 3,500 million years of history and a century of research. In *Advances in Stromatolite Geobiology, Lecture Notes in Earth Sciences*. Berlin, Heidelberg: Springer, pp. 29–74.

Roberson, A.L., Roadt, J., Halevy, I. and Kasting, J.F. (2011) Greenhouse warming by nitrous oxide and methane in the Proterozoic Eon. *Geobiology*, *9*, 313–320.

Saenger, C., Affek, H.P., Felis, T., Thiagarajan, N., Lough, J.M. and Holcomb, M. (2012) Carbonate clumped isotope variability in shallow water corals: temperature dependence and growth-related vital effects. *Geochimica et Cosmochimica Acta*, *99*, 224–242.

Schoell, M. (1984) Recent advances in petroleum isotope geochemistry. *Organic Geochemistry*, *6*, 645–663.

Sheldon, N.D. (2006) Precambrian paleosols and atmospheric CO_2 levels. *Precambrian Research*, *147*, 148–155.

Sheldon, N.D. (2012). Microbially induced sedimentary structures in the ca. 1100 Ma terrestrial midcontinent rift of North America. Microbial Mats in Siliciastic Depositional Systems Through Time. *SEPM Special Publication*, (11), 153–162.

Sheldon, N.D. (2013) Causes and consequences of low atmospheric pCO_2 in the late Mesoproterozoic. *Chemical Geology*, *362*, 224–231.

Shenton, B.J., Grossman, E.L., Passey, B.H., Henkes, G.A., Becker, T.P., Laya, J.C., et al. (2015) Clumped isotope thermometry in deeply buried sedimentary carbonates: the effects of bond reordering and recrystallization. *Geological Society of America Bulletin*, *127*, 1036–1051.

Shields, G. and Veizer, J. (2002). Precambrian marine carbonate isotope database: version 1.1. *Geochemistry, Geophysics, Geosystems 3*, 1 of 12–12 of 12.

Stein, C.A., Kley, J., Stein, S., Hindle, D. and Keller, G.R. (2015) North America's midcontinent rift: when rift met LIP. *Geosphere*, *11*, 1607–1616.

Swart, P.K. (2008) Global synchronous changes in the carbon isotopic composition of carbonate sediments unrelated to changes in the global carbon cycle. *Proceedings of the National Academy of Sciences*, *105*, 13741–13745.

Taran, Y.A., Kliger, G.A. and Sevastianov, V.S. (2007) Carbon isotope effects in the open-system Fischer-Tropsch synthesis. *Geochimica et Cosmochimica Acta*, *71*, 4474–4487.

Tripati, A.K., Eagle, R.A., Thiagarajan, N., Gagnon, A.C., Bauch, H., Halloran, P.R., et al. (2010) ^{13}C–^{18}O isotope signatures and "clumped isotope" thermometry in foraminifera and coccoliths. *Geochimica et Cosmochimica Acta*, *74*, 5697–5717.

Walter, M.R., Veevers, J.J., Calver, C.R., Gorjan, P. and Hill, A.C. (2000) Dating the 840–544 Ma Neoproterozoic interval by isotopes of strontium, carbon, and sulfur in seawater, and some interpretative models. *Precambrian Research*, *100*, 371–433.

Wellman, C.H. and Strother, P.K. (2015) The terrestrial biota prior to the origin of land plants (embryophytes): a review of the evidence. *Palaeontology*, *58*, 601–627.

Wilmeth, D.T., Dornbos, S.Q., Isbell, J.L. and Czaja, A.D. (2014) Putative domal microbial structure in fluvial siliciclastic facies of the Mesoproterozoic (1.09 Ga) Copper Harbor Conglomerate, Upper Peninsula of Michiga, USA. *Geobiology*, *12*, 99–108.

Zhao, M., Reinhard, C.T. and Planavsky, N.J. (2017) Terrestrial methane fluxes and Proterozoic climate. *Geology*, *46*, 139–142.

SUPPORTING INFORMATION

Additional supporting information may be found online in the Supporting Information section at the end of the article.

How to cite this article: Hren MT, Sheldon ND. Terrestrial microbialites provide constraints on the mesoproterozoic atmosphere. *Depositional Rec*. 2020;6:4–20. https://doi.org/10.1002/dep2.79